Berger, W.H., Kroenke, L.W., Mayer, L.A., et al., 1993
Proceedings of the Ocean Drilling Program, Scientific Results, Vol. 130

14. WHOLE-ROCK OXYGEN AND CARBON ISOTOPE STRATIGRAPHY OF THE PALEOGENE AND CRETACEOUS/TERTIARY BOUNDARY IN HOLE 807C[1]

Richard M. Corfield[2] and Julie E. Cartlidge[2]

ABSTRACT

Whole-rock $\delta^{18}O$ analyses of the Paleogene and Upper Cretaceous succession at Ocean Drilling Program Hole 807C suggest the presence of hiatuses between 876.95 and 894.47 mbsf and between 1138.82 and 1140.94 mbsf. The $\delta^{13}C$ data show a pronounced positive excursion between 1130 and 1180 mbsf that corresponds to the positive $\delta^{13}C$ values characteristic of the Paleocene. Despite the stratigraphic breaks in the section, the $\delta^{18}O$ data show a systematic increase between 1360 mbsf and the hiatus between 876.95 and 894.47 mbsf, which is consistent with previous suggestions of long-term climatic cooling through the Paleogene. The Cretaceous/Tertiary transition is apparently complete in this section and is of remarkable thickness. The expanded nature of this portion of the succession is probably the result of secondary depositional processes. High-resolution sampling across this boundary may reveal detailed structure of the $\delta^{13}C$ decline associated with the extinctions that mark the termination of the Cretaceous.

INTRODUCTION

Ocean Drilling Program (ODP) Leg 130 Holes 807A and 807C together form a composite section penetrating Neogene, Paleogene, and Cretaceous sediments on the flank of the Ontong Java Plateau. The upper part of the section consists of foraminiferal and nannofossil chalk that grades into limestone at approximately 1000 m below sea floor (mbsf). We made whole-rock $\delta^{13}C$ and $\delta^{18}O$ measurements throughout the Paleogene and Cretaceous intervals of this section to assist in the identification of stratigraphic breaks and the documentation of paleoceanographic trends. In particular, we concentrated on the Cretaceous/Tertiary transition. The lithified nature of the Paleogene and Cretaceous does not presage well for detailed Cretaceous/Tertiary boundary studies in comparison with such sites as Deep Sea Drilling Project (DSDP) Site 577 (Zachos et al., 1985) or Hole 690B (Stott and Kennett, 1990). However, Hole 807C was drilled in a graben, and, as shown in this study, the unique sedimentological setting of this site may yield an exceptionally detailed record of the Cretaceous/Tertiary boundary transition.

METHODS

The $\delta^{13}C$ and $\delta^{18}O$ stratigraphies generated by the analysis of whole-rock samples were used to identify discontinuities that might be a result of the presence of hiatuses. Samples were drilled from limestone chips using a vibrotool, cleaned using 10% hydrogen peroxide and acetone, and then dried for 30 min at 60°C. The samples were analyzed isotopically using a VG Isotech PRISM mass spectrometer with an on-line VG Isocarb carbonate preparation system in the Oxford laboratory. The mass spectrometer is calibrated to PDB daily by means of an in-house carbonate standard (NOCZ), which is calibrated regularly to NBS 19. Reproducibility of replicate standards was better than 0.1‰.

RESULTS AND DISCUSSION

Figure 1 shows the $\delta^{13}C$ and $\delta^{18}O$ whole-rock stratigraphy of the composite Paleogene section of Holes 807A and 807C (data in Appendix). The $\delta^{18}O$ record in particular is useful for the identification of hiatuses because of its systematic change over the interval from the base of the measured section (1360 mbsf) to a major discontinuity between 876.95 and 894.47 mbsf (Samples 130-807C-12R-1, 35–37 cm, and -15R-1, 57–59 cm). This generally monotonic trend is probably the local expression of the long-term Cenozoic cooling documented in foraminifers by previous authors (e.g., Savin, 1977; Corfield et al., 1991). The discontinuity marked "A" between 876.95 and 894.47 mbsf is not obviously connected to evidence of a hiatus from the shipboard biostratigraphy (Shipboard Scientific Party, 1991), but this may be because of the relative scarcity of biostratigraphic datums within this interval of the core. Also, this level in Hole 807C is characterized by poor recovery of sediment.

Another discontinuity (marked "B") occurs in the $\delta^{18}O$ record between 1138.82 and 1140.9 mbsf (between Samples 130-807C-46R-3, 62–64 cm, and -47R-1, 70–72 cm). Shipboard biostratigraphic data do not suggest the presence of a hiatus at this level in the hole. However, this may be caused by the difficulties of assigning age determinations in limestone with a low abundance of marker species.

The interval between 1138.82 and 1188.8 mbsf (130-807C-46R-3, 62–64 cm) and 1180 mbsf (130-807C-54R-1, 0–2 cm) exhibits very positive $\delta^{13}C$ values. This interval is within the Paleocene, as determined by the shipboard biostratigraphers, and the isotopically positive values are entirely typical of this interval (Shackleton and Hall, 1984; Shackleton et al., 1985; Stott et al., 1990; Corfield et al., 1991). Figure 2 illustrates this portion of the core in more detail as well as the Cretaceous/Tertiary boundary and the Late Cretaceous.

Premoli Silva (this volume) has identified a stratigraphic break (marked "C" on Fig. 2) between planktonic foraminiferal Zones P11 and P5 between 1160.24 and 1161.26 mbsf (between Samples 130-807C-51R-1, 3–5 cm, and -51R-1, 105–107 cm). Our $\delta^{13}C$ data do not unequivocally support this interpretation however. The $\delta^{13}C$ signal across this portion of the core shows the monotonic decline characteristic of the upper Paleocene/Paleocene-Eocene boundary interval. The gap suggested by the biostratigraphy of Premoli Silva is approximately 10 m.y. (between 58 and 48 Ma) using the time scale of Berggren et al. (1985). This interval is characterized by a $\delta^{13}C$ decline toward the $\delta^{13}C$ minimum at or near the Paleocene/Eocene boundary, followed by a recovery to values intermediate between the ^{13}C maximum of the late Paleocene and the minimum near the Paleocene/Eocene boundary. The whole-rock $\delta^{13}C$ stratigraphy from DSDP 527 illustrated by Shackleton et al. (1985, fig. 4) shows that at 48 Ma $\delta^{13}C$ values were at about approximately 2‰; 10 m.y. earlier (at 58 Ma) $\delta^{13}C$ values from the same site were similar. Hence, no unique $\delta^{13}C$ value for this interval is present that would discriminate

[1] Berger, W.H., Kroenke, L.W., Mayer, L.A., et al., 1993. *Proc. ODP, Sci. Results,* 130: College Station, TX (Ocean Drilling Program).

[2] Department of Earth Sciences, University of Oxford, Park's Road, Oxford OX1 3PR, United Kingdom.

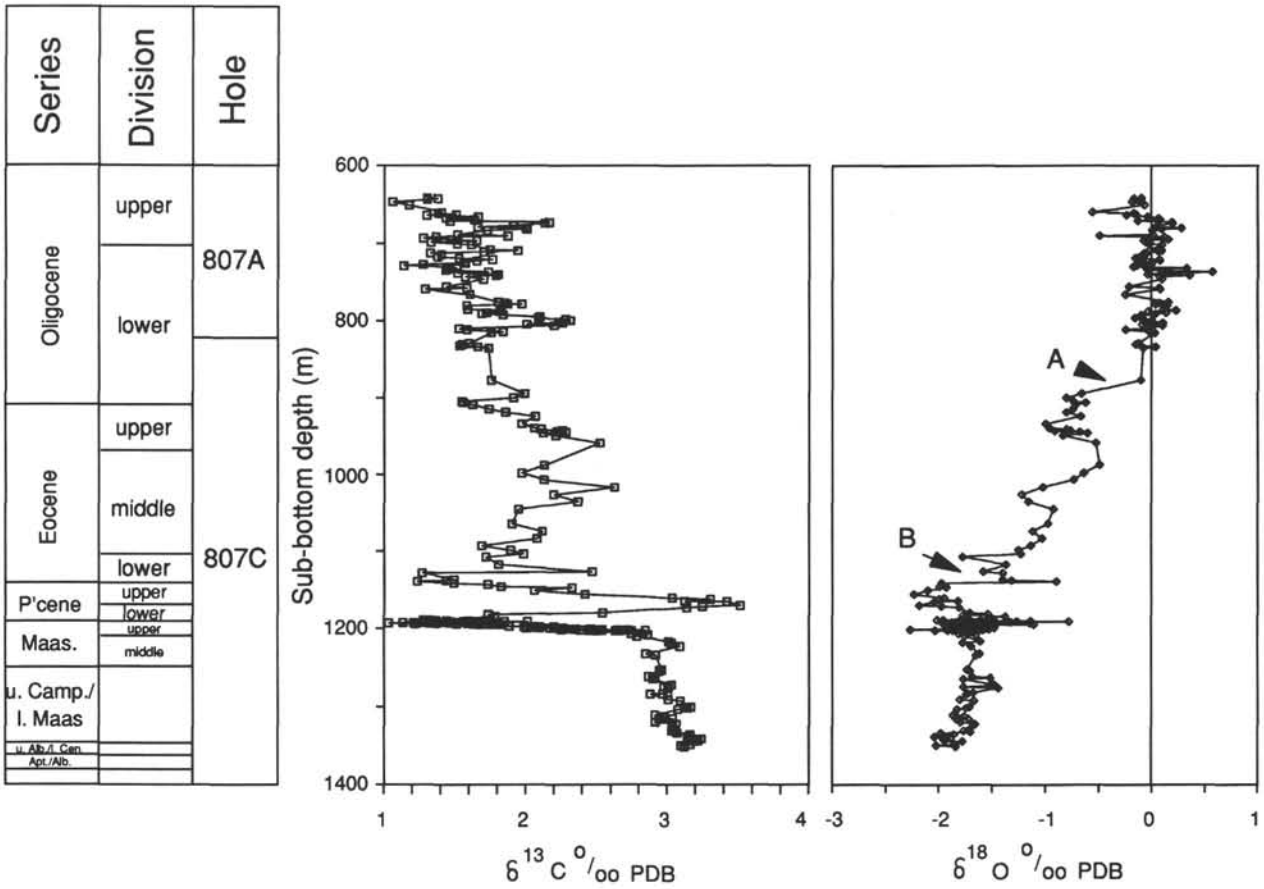

Figure 1. Oxygen and carbon isotope stratigraphy of the Paleogene and Cretaceous of Holes 807A and 807C. A = possible hiatus between 876.95 and 894.47 mbsf, B = possible hiatus between 1138.82 and 1188.8 mbsf.

between the two possibilities. However, as Figure 1 shows, $\delta^{13}C$ values continue to decline after the interval between Samples 130-807C-51R-1, 3–5 cm, and -51R-1, 105–107 cm. This decline may be the local manifestation of the continuing $\delta^{13}C$ decrease known from other sections to be characteristic of the early Eocene. If this is the case, then it is unlikely that the biostratigraphic assignment of sediments up to 1127.24 (Sample 130-807C-45R-2, 64 cm) where the possible hiatus marked "B" occurs, are really from planktonic foraminifer biozones P11 through P12/P13. This discrepancy may be reconciled by the fact that this portion of Hole 807C is known to be heavily reworked (Fig. 1; Premoli Silva, this volume); and, as she points out, because of the pervasive resedimentation in this part of the hole, zonal assignments are tentative. The $\delta^{18}O$ data also fail to show a discontinuity at this level that might support the presence of a hiatus.

Premoli Silva (this volume) also suggests the possibility of a hiatus (marked "D" on Fig. 2) between 1184.49 and 1185.51 mbsf between planktonic foraminiferal Zone P3 and Subzone P1b (Samples 130-807C-53R-4, 58–60 cm, and -53R-5, 10–12 cm). Both the $\delta^{13}C$ and the $\delta^{18}O$ data indicate a disjunction that might support this hypothesis. Further biostratigraphic and chemostratigraphic work at a higher sample spacing is clearly required to resolve these differences.

The Cretaceous/Tertiary Boundary at Hole 807C

We significantly increased our sampling resolution across the Cretaceous/Tertiary boundary at Hole 807C based on the identification by shipboard biostratigraphers of the *Thoracosphaera* bloom that is characteristic of the immediate aftermath of the boundary interval (Pospichal and Wise, 1990). In addition, we used the biostratigraphic data of Premoli Silva (this volume), which provides further constraints on the stratigraphy of this portion of Hole 807C. Premoli Silva (this volume) places the Cretaceous/Tertiary boundary between Samples 130-807C-55R-1, 49–50 cm, and -55R-1, 35–36 cm (1197.39 and 1197.25 mbsf) on the basis of the first occurrence (FO) of Tertiary planktonic foraminifers. Hence, a median estimate of the position of this boundary is at Sample 130-807C-55R-1, 42–43 cm (1197.32 mbsf). Premoli Silva (this volume) further estimates the FO of *Subbotina pseudobulloides* (which according to the zonal scheme of Berggren and Miller [1988] defines the base of planktonic foraminifer Subzone P1a) to lie at Sample 130-807C-54R-4, 148–149 cm (1194.78 mbsf). This is consistent with the placement by Mao and Wise (this volume) of the FO of *Coccolithus pelagicus* (within nannofossil Subzone CP1b) at Sample 130-54R-3, 90 cm (1192.7 m). Using the FO of Danian planktonic foraminifera and the FO of *S. pseudobulloides*, we calculate a median thickness for this interval of 2.54 m. Using the time scale of Berggren et al. (1985), this yields a sedimentation rate for this part of Hole 807C of 12.7 m/m.y. We note, however (Premoli Silva, this volume), that problems exist in unequivocally assigning zonal boundaries because of the lithified nature of the sediment. As Table 1 shows, this is the highest sedimentation rate documented of several intensively studied Cretaceous/Tertiary boundary sections, with the possible exception of DSDP Site 524 (Hsü et al., 1982). We note that our sedimentation rate estimate of 12.7 m/m.y. for the Cretaceous/Tertiary transition at Hole 807C is similar to the independent estimate of 14 m/m.y. based on paleomagnetic data (J.A. Tarduno, pers. comm., 1992; Corfield et al., this volume). Thus, although Hole 807C is in limestone facies, the potential to resolve closely spaced chemostratigraphic and biostratigraphic events exists at this site, provided it can be demonstrated that the sediments have not been too distorted by secondary sedimentation.

Figure 3 illustrates our $\delta^{13}C$ and $\delta^{18}O$ data from the Cretaceous/Tertiary boundary interval at Hole 807C. The $\delta^{13}C$ decline noted by

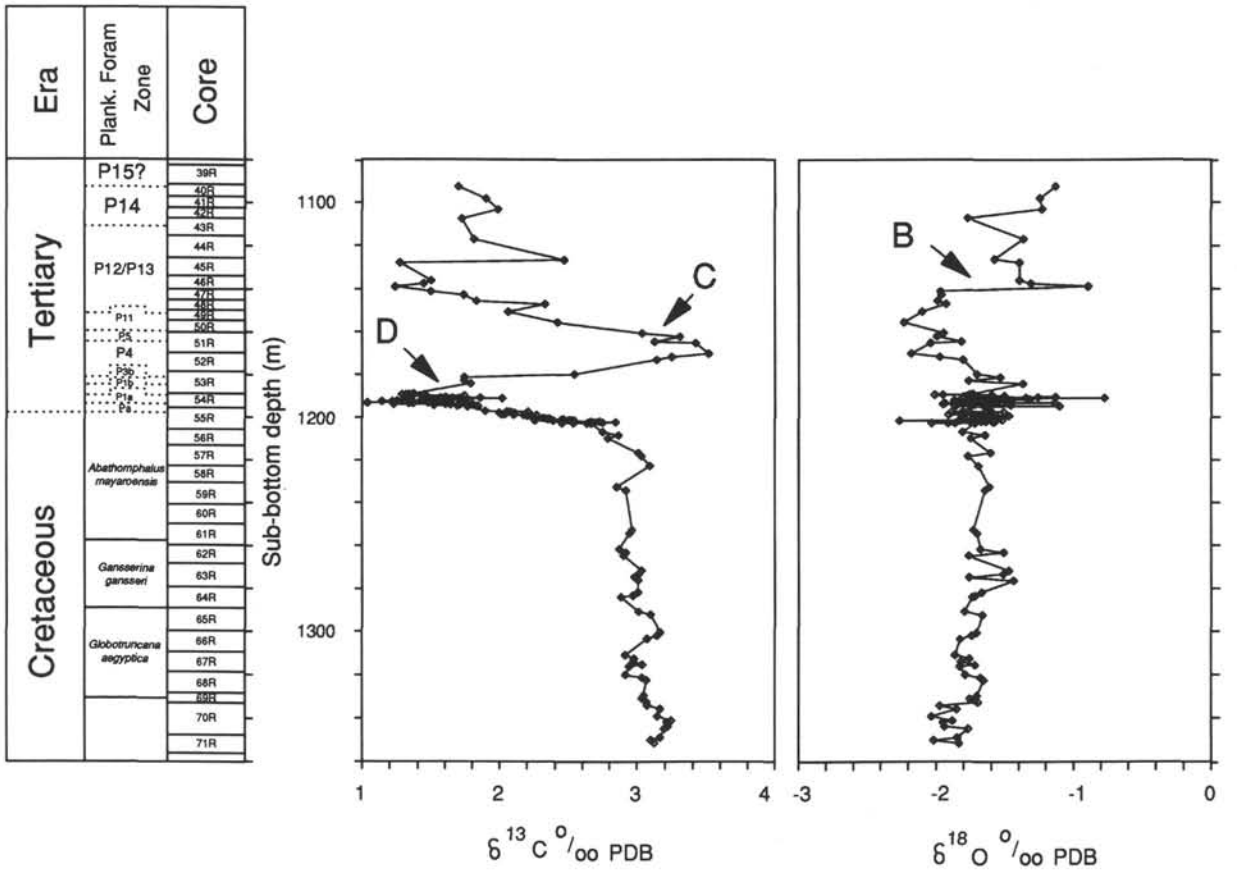

Figure 2. Oxygen and carbon isotope stratigraphy of the Paleocene and Upper Cretaceous of Hole 807C. Note the isotopically positive values characteristic of the Paleocene epoch. Hiatus B is identified; C and D = possible hiatuses inferred from lack of identifiable foraminiferal zones (Premoli Silva, this volume).

authors at several different sites (e.g., Scholle and Arthur [1980], Renard [1986], and Corfield et al. [1991] at the Bottaccione Gorge section in Italy; Shackleton and Hall [1984] at DSDP Site 527; Zachos and Arthur [1986] at DSDP 577; Stott and Kennett [1990] at ODP Hole 690B) is clearly discernible at Hole 807C. In addition, because of the high sedimentation rates in the Cretaceous/Tertiary boundary interval at Hole 807C, the $\delta^{13}C$ decline occurs over a thickness of 9.23 m. This is probably the most expanded Cretaceous/Tertiary $\delta^{13}C$ decline yet documented.

Clearly, it is imperative to understand how such a thick Cretaceous/Tertiary boundary section could have been deposited and whether such a section can be regarded as stratigraphically continuous and sedimentologically undisturbed. The high sedimentation rates calculated for the Cretaceous/Tertiary boundary interval at Hole 807C strongly suggest that deposition was not primary. W.H. Berger (pers. comm., 1991) has suggested that sedimentation rates at Hole 807C were significantly enhanced during this interval as a result of winnowing of the sediment cover surrounding the graben. The increased flux of sediment into the graben would result in significantly higher sedimentation rates because of the confined nature of this small sedimentary basin. Support for this hypothesis comes from the biostratigraphic data of Premoli Silva (this volume) and Sliter and Leckie (this volume), who identified both size and shape sorting of planktonic foraminifers from thin sections that suggest winnowing. As well as size and shape sorting, Premoli Silva (this volume) has identified turbiditic layers within the Cretaceous/Tertiary succession at Hole 807C. We have plotted these intervals of sedimentological disturbance on Figure 3. The setting of the Cretaceous/Tertiary boundary at this site is further discussed in Corfield et al. (this volume).

In addition to this peculiar sedimentological environment, evidence is present for stylolitization within this portion of Hole 807C. The sediment compression implied by stylolitization suggests the probability that carbonate-bearing pore fluids might have been mobilized, possibly leaching sediment from one part of the core and depositing it elsewhere in the form of carbonate cement. However, the presence of stylolites is patchy within the Cretaceous/Tertiary boundary section of Hole 807C and is limited at most to centimeter-scale occurrence. Thus, we consider it unlikely that this process could have affected the whole 9.23-m thickness of the $\delta^{13}C$ decline at the Cretaceous/Tertiary boundary at Hole 807C. Diagenetic complications of the $\delta^{13}C$ signal are further discussed in Corfield et al. (this volume).

Given the pervasive influence of foraminiferal resedimentation from winnowing and turbidity currents within the boundary interval at Hole 807C, it is possible that the monotonic decline in $\delta^{13}C$ over this 9.23-m interval is a result at least in part of secondary depositional processes, and therefore that the record is not a reliable portrait of events. Reworking of fine-fraction calcite could result theoretically in the transposition of heavy (Cretaceous) $\delta^{13}C$ values to higher (Danian) levels in the core if the ratio of reworked material to material in primary position were high and the reworked material were significantly older than the primary material. To rework the entire 9.23-m thickness of the Cretaceous/Tertiary boundary carbon isotope depletion at Hole 807C would require the mixing of older material relatively enriched in ^{13}C with younger material relatively depleted in ^{13}C, and its amalgamation into micrite, which would possess an average $\delta^{13}C$ composition. We note, however, that the $\delta^{13}C$ record across the Cretaceous/Tertiary boundary at Hole 807C proceeds remarkably uniformly, a feature not necessarily predicted by the episodic rework-

Table 1. Comparative sedimentation rates across selected DSDP and ODP Cretaceous/Tertiary boundary sections.

Hole	Sedimentation rate (m/m.y.)
DSDP 577	[1]1.95
DSDP 524	[2]66.60
DSDP 527	[3]5.00
ODP 690C	[4]2.50*
ODP 689B	[4]1.00*
ODP 807C	12.70

Notes: Estimates based on depth difference between the Cretaceous/ Tertiary boundary and the FO of *Subbotina pseudo-bulloides* (K/T boundary in this case is defined by the FO of Danian planktonic foraminifers except where marked with an asterisk (*), in which case the boundary is defined by the LO of Cretaceous planktonic foraminifers).

[1] Date from Gerstel et al. (1986), but also see discussion by Corfield and Shackleton (1988).

[2] This high value is almost certainly the result of the poor depth uncertainties associated with the planktonic foraminifer age control points over this interval in DSDP Hole 524. Note, however, that Hsü et al. (1982) claimed very high rates of 30 m/m.y. for this site on the basis of other sedimentation rate constraints.

[3] Data from Boersma (1984).

[4] Data from Thomas et al. (1990).

ing of older material suggested by size and shape sorting of foraminifers. In addition, if secondary sedimentation from the region around the graben walls occurred contemporaneously with primary sedimentation, as is conceivable from the winnowing and bottom-current activity suggested for this site, then there is no reason to suppose that the overall features of the $\delta^{13}C$ decline would be lost. Clearly, the data at present are insufficient to distinguish the relative contributions to the $\delta^{13}C$ decline of primary and secondary sedimentation across the Cretaceous/Tertiary boundary at Hole 807C. As a check on the reproducibility of our data, we have repeated some measurements over the $\delta^{13}C$ minimum as well as replicating five additional times selected measurements over the entire $\delta^{13}C$ decline (Tables 2 and 3). Both types of repeat analyses show good agreement (Fig. 4) with our original measurements, confirming the expanded nature of this Cretaceous/Tertiary boundary $\delta^{13}C$ decline at Hole 807C.

Figure 3 shows that the initiation of the most rapid $\delta^{13}C$ decline occurs at 1202.25 mbsf (Sample 130-807C-55R-4, 85–87 cm). This is significantly below the FO of Tertiary planktonic foraminifers, which occurs at 1197.32 mbsf (Sample 130-807C-55R-1, 42–43 cm). The $\delta^{13}C$ values continue to decline with minor fluctuations, reaching a minimum at 1193.02 mbsf (Sample 130-807C-54R-3, 122–124 cm). This is coincident with the peak in the *Thoracosphaera* bloom noted by the shipboard biostratigraphers (Shipboard Scientific Party, 1991) and initially used to locate the position of the Cretaceous/Tertiary boundary at Hole 807C. The amplitude of the $\delta^{13}C$ decline between 1202.25 and 1193.02 mbsf is 1.7‰. If secondary sedimentation was pervasive during the deposition of this boundary succession, then the stratigraphic separation of the onset of $\delta^{13}C$ decline and the last occurrence (LO) of Cretaceous planktonic foraminifers and Cretaceous nannofossils could be caused by the reworking of these fossils higher up the section. However, the Cretaceous/Tertiary boundary has been placed on the FO of Danian planktonic foraminifers between Samples 130-807C-55R-1, 49–50 cm, and -55R-1, 35–36 cm (1197.39 and 1197.25 mbsf; median = 1197.32). It is difficult to explain the separation of the onset of $\delta^{13}C$ decline and the *first occurrence* of Danian planktonic foraminifers by reworking. Hence, this separation must be considered a primary phenomenon in the absence of data to the contrary.

The $\delta^{18}O$ data remain relatively constant over the interval between 1202.5 mbsf (Sample 130-807C-55R-4, 110 cm) and 1196.97 mbsf (Sample 130-807C-55R-1, 7–8 cm). After an interval of no recovery (placed by ODP convention at the base of the core barrel), $\delta^{18}O$ values are about 0.1‰ more negative at –1.8‰. At 1193.02 mbsf, coincident with the peak in the *Thoracosphaera* bloom, $\delta^{18}O$ values begin to increase. The $\delta^{18}O$ increase peaks at 1190.26 mbsf (Sample 130-807C-54R-1, 146–148 cm) and its amplitude is 0.6‰. Recrystallization is widespread within this section, and it is impossible, therefore, to make specific assertions about absolute change in temperature. In particular, the $\delta^{18}O$ values are relatively negative (in general, fluctuating around –1.8‰) compared with other important Cretaceous/Tertiary boundary successions from the deep ocean. Whole-rock or fine-fraction measurements from DSDP Holes 47.2 and 577 (Zachos et al., 1985) fluctuate around approximately –1‰, whereas fine-fraction measurements from a depth transect of Cretaceous/Tertiary boundary sites drilled during DSDP Leg 74 (Shackleton and Hall, 1984) are in the 0.0‰ to about –0.5‰ range. As DSDP Hole 577 was in the tropics during the Late Cretaceous and Paleocene, these fine-fraction values may be considered to reflect sea-surface temperatures as monitored predominantly by nannofossils. Our more negative results from Hole 807C are therefore likely to be the result of recrystallization at relatively elevated deep burial temperatures. However, recrystallization in the absence of conspicuous quantities of organic matter is unlikely to have significantly modified the shape of the $\delta^{13}C$ decline (e.g., Williams et al., 1988).

Our data show that the beginning of the $\delta^{13}C$ decrease precedes the FO of Tertiary planktonic foraminifers, but that the apparent onset of the $\delta^{13}C$ decline may be more or less synchronous with the beginning of the Cretaceous/Tertiary boundary interval as recognized using nannofossils (Mao and Wise, this volume). We note, however, that the position of the Cretaceous/Tertiary boundary is difficult to place precisely because of poor preservation and reworking.

If we assume that the apparent separation of the FO of Tertiary planktonic foraminifers and the onset of $\delta^{13}C$ decline is a primary feature of the record at Hole 807C, then it is useful to attempt to constrain the relative timing of events. We have developed a time scale for this interval of Hole 807C (Fig. 5), and our estimates suggest that the onset of the $\delta^{13}C$ decline precedes the extinction by 450,000 yr. Note that this is certainly an overestimate due to the use of the *S. pseudobulloides* datum in a reworked succession. Other workers have shown that the $\delta^{13}C$ decline preceded the extinction of the planktonic foraminifers (e.g., at neritic sites exposed in Europe [Perch-Nielson et al., 1982] and at DSDP 524 [Hsü et al., 1982]). Hence, it is not surprising that in the expanded section recovered at Hole 807C this feature should also be distinguished.

Macleod and Keller (1991) have recently pointed out that the apparent rapidity of the $\delta^{13}C$ decline at the Cretaceous/Tertiary boundary in deep-sea sections may be a result of the widespread occurrence of hiatuses across the boundary interval. The implication, therefore, is that if the $\delta^{13}C$ decline is gradual then the probability exists that the boundary is more complete than where the $\delta^{13}C$ decline is abrupt. It is an unfortunate feature of the Cretaceous/Tertiary boundary section at Hole 807C that at present the nannofossil biostratigraphy is inadequate to accurately constrain the precise sequence of floral events with respect to the $\delta^{13}C$ curve. Given the reservations of Mao and Wise (this volume) concerning the poor preservation and reworking of nannofossils across this Cretaceous/Tertiary boundary succession, it may well be that further refinement of the nannofossil biostratigraphy is not possible. It is clear, however, that the $\delta^{13}C$ decline and the FO of Tertiary planktonic foraminifers occurs before the *Thoracosphaera* bloom. This is consistent with the hypothesis that the *Thoracosphaera* bloom was a response to vacated ecospace (the "Strangelove Ocean" of Hsü and McKenzie, 1985).

We conclude that the unique sedimentological setting of Hole 807C has led to the recovery of an apparently complete record of the $\delta^{13}C$ change across the Cretaceous/Tertiary boundary event, although the succession contains a significant component from resedimentation. We note, however, that reworking was apparently

pervasive at the relatively thick Cretaceous/Tertiary boundary section at DSDP Site 527 without markedly deforming the $\delta^{13}C$ decline across the Cretaceous/Tertiary boundary there. However, those measurements were made on unlithified samples and were relatively unaffected by the problems of secondary cementation noted in Hole 807C.

ACKNOWLEDGMENTS

We are grateful to Isabella Premoli Silva and Bill Sliter for making available their planktonic foraminiferal biostratigraphy of the Cretaceous/Tertiary boundary interval in Hole 807C. We thank John Tarduno for making available his paleomagnetic data for the Cretaceous/Tertiary interval in Hole 807C. We are also grateful to Mike Durkin for valuable and stimulating discussion and for reading earlier versions of this manuscript. Finally, we are sincerely grateful to Lowell Stott and Jim Zachos for careful and constructive reviews of this paper, which substantially improved the final version.

REFERENCES*

Berggren, W.A., Kent, D.V. and Flynn, J.J., 1985. Jurassic to Paleogene: Part 2. Paleogene geochronology and chronostratigraphy. *In* Snelling, N.J. (Ed.), *The Chronology of the Geological Record.* Geol. Soc. London Mem., 10:141–195.

Berggren, W.A., and Miller, K.G., 1988. Paleogene tropical planktonic foraminiferal biostratigraphy and magnetobiochronology. *Micropaleontology,* 34:362–380.

Boersma, A., 1984. Cretaceous-Tertiary planktonic foraminifers from the southeastern Atlantic, Walvis Ridge area, Deep Sea Drilling Project Leg 74. *In* Moore, T.C., Jr., Rabinowitz, P.D., et al., *Init. Repts. DSDP,* 74: Washington (U.S. Govt. Printing Office), 501–524.

Corfield, R.M., Cartlidge, J.E., Premoli Silva, I., and Housley, R.A., 1991. Oxygen and carbon isotope stratigraphy of the Paleogene and Cretaceous limestones in the Bottaccione Gorge and the Contessa Highway sections, Umbria, Italy. *Terra Nova,* 3:414–422.

Corfield, R.M., and Shackleton, N.J., 1988. Comment and reply on "Danian faunal succession: planktonic foraminiferal response to a changing marine environment." *Geology,* 16:378–379.

Gerstel, J., Thunell, R.C., Zachos, J.C., and Arthur, M.A., 1986. The Cretaceous/Tertiary boundary events in the North Pacific: planktonic foraminiferal results from Deep Sea Drilling Project Site 577, Shatsky Rise. *Paleoceanography,* 1:97–117.

Hsü, K.J., He, Q., McKenzie, J.A., Weissert, H., Perch-Nielson, K., Oberhänsli, H., Kelts, K., LaBrecque, J., Tauxe, L., Krähenbühl, U., Percival, S.F., Wright, R., Karpoff, A.M., Petersen, N., Tucker, P., Poore, R.Z., Gombos, A.M., Pisciotto, K., Carman, M.F., Schreiber, E., 1982. Mass mortality and its environmental and evolutionary consequences. *Science,* 216:249–256.

Hsü, K.J., and McKenzie, J.A., 1985. A "strangelove" ocean in the earliest Tertiary. *In* Sundquist, E.T., and Broecker, W.S. (Eds.), *The Carbon Cycle and Atmospheric CO_2: Natural Variations Archean to Present.* Am. Geophys. Union, Geophys. Monogr., 32:487–492.

Macleod, N., and Keller, G., 1991. Hiatus distributions and mass extinctions at the Cretaceous/Tertiary boundary. *Geology,* 19:497–501.

Perch-Nielson, K., McKenzie, J., and He, Q., 1982. Biostratigraphy and isotope stratigraphy and the "catastrophic" extinction of calcareous nannoplankton at the Cretaceous/Tertiary boundary. *In* Silver, L.T., and Schultz, P.H. (Eds.), *Geological Implications of Impacts of Large Asteroids and Comets on the Earth.* Spec. Pap., Geol. Soc. Am., 190:353–371.

Pospichal, J.J., and Wise, S.W., Jr., 1990. Calcareous nannofossils across the K/T boundary, ODP Hole 690C, Maud Rise, Weddell Sea. *In* Barker, P.F., Kennett, J.P., et al., *Proc. ODP, Init. Repts.,* 113: College Station, TX (Ocean Drilling Program), 515–532.

Renard, M., 1986. Pelagic carbonate chemostratigraphy (Sr, Mg, ^{18}O, ^{13}C). *Mar. Micropaleontol.,* 10:117–164.

Savin, S.M., 1977. The history of the Earth's surface temperature during the past 100 million years. *Annu. Rev. Earth. Planet. Sci.,* 5:319–355.

Scholle, P.A., and Arthur, M.A., 1980. Carbon isotope fluctuations in Cretaceous pelagic limestones: potential stratigraphic and petroleum exploration tool. *AAPG Bull.,* 64:67–87

Shackleton, N.J., and Hall, M.A., 1984. Carbon isotope data from Leg 74 sediments. *In* Moore, T.C., Jr., Rabinowitz, P.D., et al., *Init. Repts. DSDP,* 74: Washington (U.S. Govt. Printing Office), 613–619.

Shackleton, N.J., Hall, M.A., and Bleil, U., 1985. Carbon isotope stratigraphy, Site 577. *In* Heath, G.R., Burckle, L.H., et al., *Init. Repts. DSDP,* 86: Washington (U.S. Govt. Printing Office), 503–512.

Shipboard Scientific Party, 1991. Site 807. *In* Kroenke, L.W., Berger, W.H., Janecek, T.R., et al., *Proc. ODP, Init. Repts.,* 130: College Station, TX (Ocean Drilling Program), 369–493.

Stott, L.D., and Kennett, J.P., 1990. The paleoceanographic and paleoclimatic signature of the Cretaceous/Paleogene boundary in the Antarctic: stable isotopic results from ODP Leg 113. *In* Barker, P.F., Kennett, J.P., et al., *Proc. ODP, Init. Repts.,* 113: College Station, TX (Ocean Drilling Program), 829–848.

Stott, L.D., Kennett, J.P., Shackleton, N.J., and Corfield, R.M., 1990. The evolution of Antarctic surface waters during the Paleogene: inferences from stable isotopic composition of planktonic foraminifers, ODP Leg 113. *Proc. ODP, Sci. Results,* 113: College Station, TX (Ocean Drilling Program), 849–863.

Thomas, E., Barrera, E., Hamilton, N., Huber, B.T., Kennett, J.P., O'Connell, S.B., Pospichal, J.J., Spieß, V., Stott, L.D., Wei, W., and Wise, S.W., Jr., 1990. Upper Cretaceous-Paleogene stratigraphy of Sites 689 and 690, Maud Rise, (Antarctica). *In* Barker, P.F., Kennett, J.P., et al., *Proc. ODP, Sci. Results,* 113: College Station, TX (Ocean Drilling Program), 901–914.

Williams, D.F., Lerche, I., and Full, W.E., 1988. *Isotope Chronostratigraphy:* San Diego (Academic Press).

Zachos, J.C., and Arthur, M.A., 1986. Paleoceanography of the Cretaceous/Tertiary boundary event: inferences from stable isotopic and other data. *Paleoceanography,* 1:5–26.

Zachos, J.C., Arthur, M.A., Thunell, R.C., Williams, D.F., and Tappa, E.J., 1985. Stable isotope and trace element geochemistry of carbonate sediments across the Cretaceous/Tertiary boundary at Deep Sea Drilling Project Hole 577, Leg 86. In Heath, G.R., Burckle, L.H., et al., *Init. Repts. DSDP,* 86: Washington (U.S. Govt. Printing Office), 513–532.

---

* Abbreviations for names of organizations and publication titles in ODP reference lists follow the style given in *Chemical Abstracts Service Source Index* (published by American Chemical Society).

Date of initial receipt: 9 September 1991
Date of acceptance: 1 September 1992
Ms 130B-027

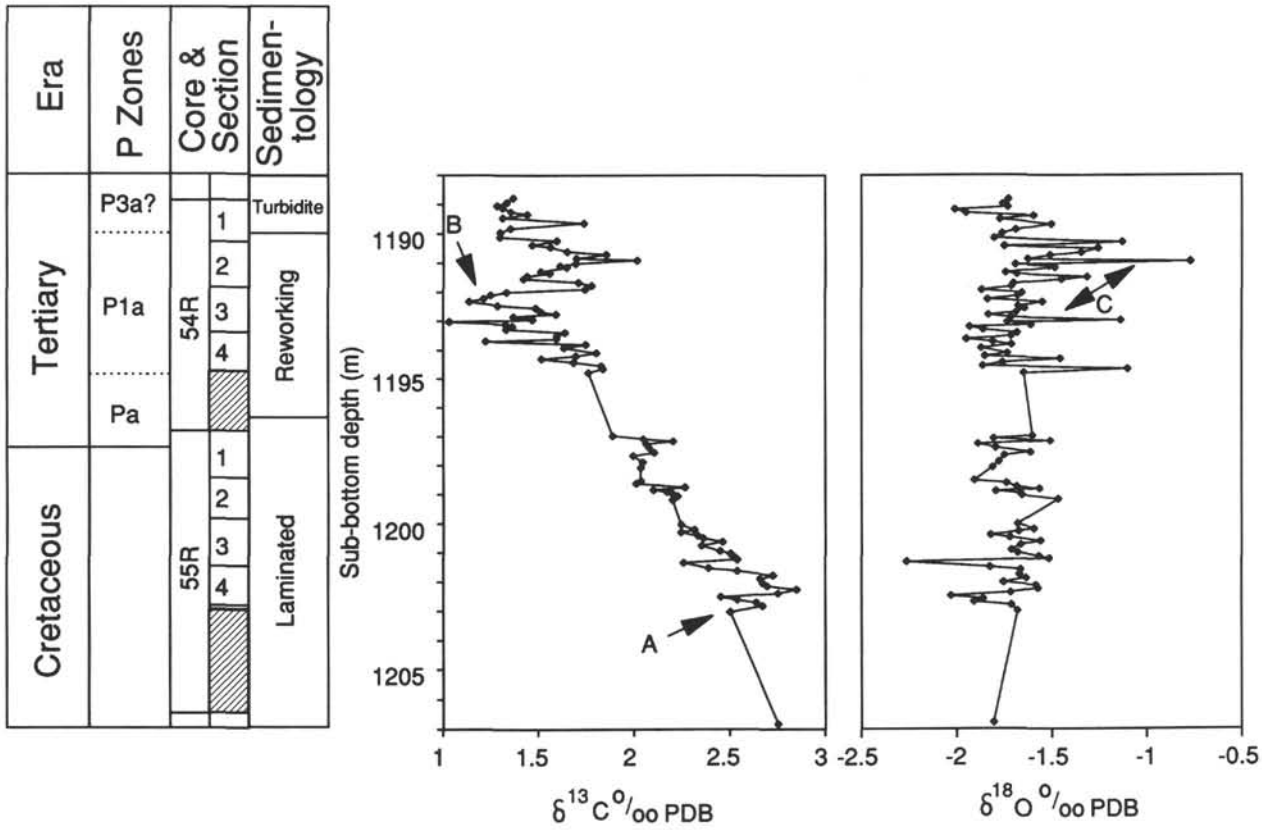

Figure 3. Oxygen and carbon isotope stratigraphy of the Cretaceous/Tertiary transition at Hole 807C with foraminiferal zones and sedimentology of Premoli Silva (this volume).

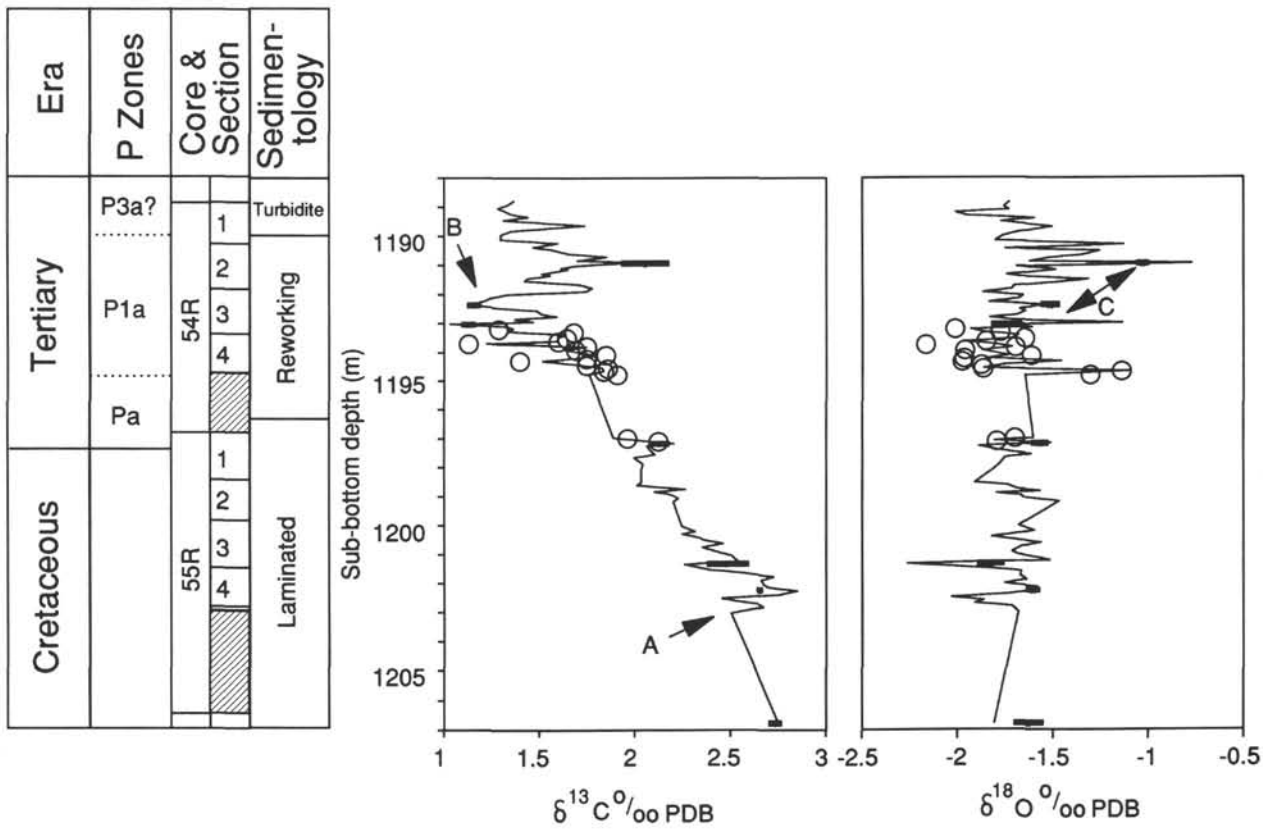

Figure 4. Repeat analyses of whole-rock carbonates across the Cretaceous/Tertiary boundary succession at Hole 807C. Circles refer to individually repeated measurements, solid bars are 1 standard deviation around the mean of 5 additional measurements of that sample.

Table 2. Repeated single measurements on selected carbonates across the $\delta^{13}C$ minimum of the Cretaceous/Tertiary boundary at Hole 807C.

Lab no.	Hole, core, section, interval (cm)	Depth (mbsf)	$\delta^{13}C$	$\delta^{18}O$	Age (Ma)
A90/2016	807C-54R-3, 139	1193.19	1.28	–2.00	66.07
A90/2017	807C-54R-3, 149	1193.29	1.68	–1.77	66.08
A90/2019	807C-54R-4, 20	1193.50	1.64	–1.64	66.10
A90/2020	807C-54R-4, 31	1193.61	1.60	–1.84	66.11
A90/2021	807C-54R-4, 40	1193.70	1.13	–2.15	66.11
A90/2022	807C-54R-4, 50	1193.80	1.75	–1.69	66.12
A90/2023	807C-54R-4, 62	1193.92	1.69	–1.95	66.13
A90/2024	807C-54R-4, 80	1194.10	1.85	–1.61	66.15
A90/2025	807C-54R-4, 90	1194.20	1.74	–1.96	66.15
A90/2026	807C-54R-4, 100	1194.30	1.39	–1.97	66.16
A90/2027	807C-54R-4, 113	1194.43	1.75	–1.87	66.17
A90/2028	807C-54R-4, 125	1194.55	1.86	–1.86	66.18
A90/2029	807C-54R-4, 135	1194.65	1.83	–1.14	66.19
A90/2030	807C-54R-4, 148	1194.78	1.91	–1.30	66.20
A90/2031	807C-55R-1, 7	1196.97	1.96	–1.69	66.37
A90/2032	807C-55R-1, 17	1197.07	2.12	–1.78	66.38

Table 3. Multiple replicates of selected carbonates across the Cretaceous/Tertiary boundary succession at Hole 807C.

Lab no.	Hole, core, section, interval (cm)	Depth (mbsf)	$\delta^{13}C$	$\delta^{18}O$	Mean $\delta^{13}C$	Mean $\delta^{18}O$	1σ $\delta^{13}C$	1σ $\delta^{18}O$
NOCZ	807C (5/8/92)	—	2.24	–1.96	2.27	–1.90	0.02	0.07
NOCZ	807C (5/8/92)	—	2.26	–1.93	—	—	—	—
NOCZ	807C (5/8/92)	—	2.29	–1.80	—	—	—	—
NOCZ	807C (5/8/92)	—	2.28	–1.90	—	—	—	—
A92/2244	807C-54R-2, 62	1190.92	2.30	–0.95	2.06	–0.99	0.14	0.04
A92/2245	807C-54R-2, 62	1190.92	2.03	–0.96	—	—	—	—
A92/2246	807C-54R-2, 62	1190.92	1.98	–1.04	—	—	—	—
A92/2247	807C-54R-2, 62	1190.92	1.98	–1.01	—	—	—	—
A92/2248	807C-54R-2, 62	1190.92	2.00	–1.00	—	—	—	—
A92/2249	807C-54R-3, 53	1192.33	1.07	–1.59	1.08	–1.52	0.04	0.05
A92/2250	807C-54R-3, 53	1192.33	1.15	–1.54	—	—	—	—
A92/2251	807C-54R-3, 53	1192.33	1.08	–1.45	—	—	—	—
A92/2252	807C-54R-3, 53	1192.33	1.05	–1.52	—	—	—	—
A92/2253	807C-54R-3, 53	1192.33	1.08	–1.49	—	—	—	—
A92/2254	807C-54R-3, 122	1193.02	1.00	–1.81	1.05	–1.76	0.04	0.09
A92/2255	807C-54R-3, 122	1193.02	1.10	–1.70	—	—	—	—
A92/2256	807C-54R-3, 122	1193.02	1.09	–1.79	—	—	—	—
A92/2257	807C-54R-3, 122	1193.02	1.04	–1.65	—	—	—	—
A92/2258	807C-54R-3, 122	1193.02	1.04	–1.86	—	—	—	—
A92/2259	807C-55R-1, 26	1197.16	2.07	–1.63	2.15	–1.57	0.05	0.05
A92/2260	807C-55R-1, 26	1197.16	2.16	–1.55	—	—	—	—
A92/2261	807C-55R-1, 26	1197.16	2.20	–1.56	—	—	—	—
A92/2262	807C-55R-1, 26	1197.16	2.11	–1.62	—	—	—	—
A92/2263	807C-55R-1, 26	1197.16	2.18	–1.52	—	—	—	—
A92/2264	807C-55R-3, 143	1201.33	2.39	–1.94	2.53	–1.85	0.12	0.08
A92/2265	807C-55R-3, 143	1201.33	2.71	–1.78	—	—	—	—
A92/2266	807C-55R-3, 143	1201.33	2.48	–1.92	—	—	—	—
A92/2267	807C-55R-3, 143	1201.33	2.56	–1.84	—	—	—	—
A92/2268	807C-55R-3, 143	1201.33	2.50	–1.79	—	—	—	—
A92/2269	807C-55R-4, 85	1202.25	2.69	–1.60	2.71	–1.62	0.02	0.04
A92/2270	807C-55R-4, 85	1202.25	2.69	–1.63	—	—	—	—
A92/2271	807C-55R-4, 85	1202.25	2.72	–1.58	—	—	—	—
A92/2272	807C-55R-4, 85	1202.25	2.72	–1.68	—	—	—	—
A92/2273	807C-55R-4, 85	1202.25	2.72	–1.59	—	—	—	—
A92/2274	807C-56R-1, 20	1206.80	2.81	–1.61	2.80	–1.64	0.04	0.08
A92/2275	807C-56R-1, 20	1206.80	2.84	–1.55	—	—	—	—
A92/2276	807C-56R-1, 20	1206.80	2.74	–1.77	—	—	—	—
A92/2277	807C-56R-1, 20	1206.80	2.78	–1.60	—	—	—	—
A92/2278	807C-56R-1, 20	1206.80	2.81	–1.67	—	—	—	—
NOCZ	807C (5/8/92)	—	2.32	–1.89	2.31	–1.85	0.01	0.05
NOCZ	807C (5/8/92)	—	2.30	–1.91	—	—	—	—
NOCZ	807C (5/8/92)	—	2.33	–1.80	—	—	—	—
NOCZ	807C (5/8/92)	—	2.31	–1.83	—	—	—	—
NOCZ	807C (5/8/92)	—	2.30	–1.81	—	—	—	—

Notes: NOCZ refers to the Oxford in-house marble standard and is included to illustrate that reproducibility of Hole 807C whole-rock carbonate samples was similar to the reproducibility of our calibrating standard.

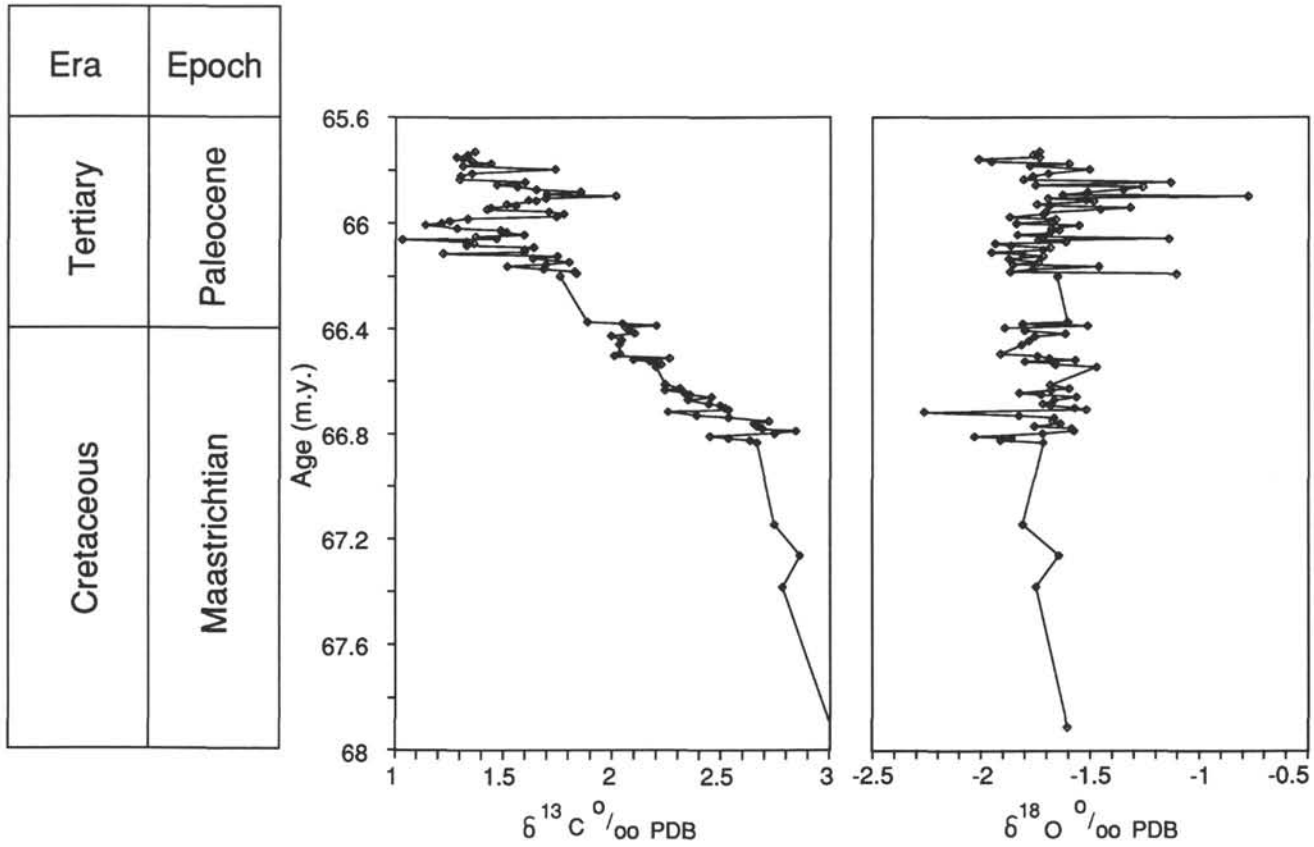

Figure 5. Oxygen and carbon isotope chronostratigraphy of the Cretaceous/Tertiary transition at Hole 807C. Note that the $\delta^{13}C$ starts at 66.85 Ma using our age estimates, and this decline precedes the first occurrence of Tertiary planktonic foraminifers (at 66.4 Ma) by 450,000 yr. Also note uncertainties in our time scale caused by the use of a foraminiferal datum (*S. pseudobulloides*) in a reworked succession.

APPENDIX

Oxygen and carbon isotope data from Holes 807A and 807C

Lab no.	Hole, core, section, interval (cm)	$\delta^{13}C$	$\delta^{18}O$	Depth (mbsf)	Age (Ma)
A90/2674	807A-68X-1, 138	1.31	–0.09	641.28	—
A90/2675	807A-68X-2, 78	1.38	–0.17	642.18	—
A90/2676	807A-68X-3, 61	1.31	–0.10	643.51	—
A90/2678	807A-68X-5, 37	1.06	–0.18	646.27	—
A90/2679	807A-69X-1, 75	1.18	–0.07	650.35	—
A90/2680	807A-70X-1, 10	1.41	–0.56	659.30	—
A90/2681	807A-70X-2, 10	1.38	–0.17	660.80	—
A90/2682	807A-70X-3, 10	1.51	–0.15	662.30	—
A90/2683	807A-70X-4, 10	1.30	–0.24	663.80	—
A90/2684	807A-70X-5, 10	1.67	–0.04	665.30	—
A90/2686	807A-70X-CC, 10	1.44	0.07	667.36	—
A90/2687	807A-71X-1, 45	1.64	0.08	669.35	—
A90/2688	807A-71X-2, 45	1.47	–0.13	670.85	—
A90/2689	807A-71X-3, 45	2.17	0.19	672.35	—
A90/2690	807A-71X-4, 45	2.13	0.20	673.85	—
A90/2692	807A-71X-CC, 45	1.92	0.05	676.85	—
A90/2693	807A-72X-1, 42	1.66	0.05	678.62	—
A90/2694	807A-72X-2, 42	2.00	0.28	680.12	—
A90/2695	807A-72X-3, 42	2.01	0.09	681.62	—
A90/2696	807A-72X-4, 42	1.73	0.01	683.12	—
A90/2697	807A-73X-1, 70	1.52	0.01	688.50	—
A90/2699	807A-73X-2, 70	1.87	–0.49	690.00	—
A90/2713	807A-73X-3, 70	1.37	0.12	691.50	—
A90/2714	807A-73X-4, 70	1.28	–0.01	693.00	—
A90/2715	807A-73X-5, 72	1.47	0.16	694.52	—
A90/2716	807A-73X-6, 70	1.66	–0.08	696.00	—
A90/2717	807A-74X-1, 92	1.33	–0.05	698.42	—
A90/2718	807A-74X-2, 92	1.52	–0.02	699.92	—
A90/2719	807A-74X-3, 92	1.62	0.10	701.42	—
A90/2720	807A-75X-1, 60	1.75	–0.01	707.80	—
A90/2721	807A-75X-2, 60	1.95	0.10	709.30	—
A90/2722	807A-75X-3, 60	1.71	0.07	710.80	—
A90/2723	807A-75X-4, 60	1.33	–0.07	712.30	—
A90/2724	807A-75X-5, 60	1.40	–0.06	713.80	—
A90/2725	807A-76X-1, 70	1.38	–0.12	717.60	—
A90/2726	807A-76X-2, 70	1.53	–0.16	719.10	—
A90/2727	807A-76X-3, 70	1.77	0.07	720.60	—
A90/2728	807A-76X-4, 70	1.66	0.08	722.10	—
A90/2729	807A-76X-5, 70	1.57	–0.09	723.60	—
A90/2730	807A-76X-6, 50	1.57	0.01	724.90	—
A90/2731	807A-77X-1, 56	1.27	–0.08	727.06	—
A90/2732	807A-77X-2, 56	1.14	–0.15	728.56	—
A90/2734	807A-77X-3, 56	1.45	–0.17	730.06	—
A90/2736	807A-77X-4, 56	1.51	0.33	731.56	—
A90/2743	807A-77X-5, 56	1.45	–0.05	733.06	—
A90/2745	807A-77X-6, 30	1.43	–0.03	734.30	—
A90/2746	807A-78X-1, 56	1.74	0.57	736.76	—
A90/2747	807A-78X-2, 56	1.52	0.09	738.26	—
A90/2748	807A-78X-3, 56	1.81	–0.04	739.76	—
A90/2749	807A-78X-4, 56	1.79	0.36	741.26	—
A90/2750	807A-78X-5, 56	1.57	0.07	742.76	—
A90/2751	807A-79X-1, 55	1.70	0.10	746.05	—
A90/2752	807A-80X-1, 53	1.44	–0.21	755.73	—
A90/2753	807A-80X-2, 55	1.59	0.07	757.25	—
A90/2754	807A-80X-3, 55	1.29	0.08	758.75	—
A90/2755	807A-81X-1, 61	1.61	–0.25	765.51	—
A90/2756	807A-82X-1, 75	1.81	0.16	775.25	—
A90/2757	807A-82X-2, 75	1.86	0.07	776.75	—
A90/2758	807A-82X-3, 77	1.87	0.04	778.27	—
A90/2759	807A-82X-3, 79	1.98	0.04	778.29	—
A90/2760	807A-82X-4, 79	1.58	0.15	779.79	—
A90/2761	807A-83X-1, 60	1.59	0.11	784.80	—
A90/2762	807A-83X-2, 60	1.83	0.23	786.30	—
A90/2763	807A-83X-3, 60	1.82	–0.03	787.80	—
A90/2764	807A-83X-4, 60	1.73	0.14	789.30	—
A90/2765	807C-2R-1, 73	1.69	0.04	790.43	—
A90/2766	807C-2R-2, 73	1.84	–0.10	791.93	—
A90/2767	807A-84X-1, 60	2.10	–0.11	794.50	—
A90/2768	807A-84X-2, 60	2.09	–0.16	796.00	—
A90/2769	807A-84X-3, 60	2.29	–0.07	797.50	—
A90/2770	807A-84X-4, 60	2.32	0.00	799.00	—
A90/2879	807A-84X-5, 60	2.24	–0.01	800.50	—
A90/2880	807A-84X-6, 60	2.26	0.11	802.00	—
A90/2881	807A-85X-1, 60	2.01	–0.09	804.20	—
A90/2882	807A-85X-2, 60	2.20	0.10	805.70	—
A90/2771	807C-4R-1, 73	1.53	–0.06	809.73	—
A90/2773	807C-4R-2, 73	1.59	–0.24	811.23	—
A90/2774	807A-86X-1, 60	1.84	–0.02	813.80	—
A90/2878	807A-86-2, 60	1.76	0.03	815.30	—
A90/2775	807C-6R-1, 73	1.60	–0.12	829.03	—
A90/2776	807C-6R-2, 73	1.55	–0.15	830.53	—
A90/2777	807C-6R-3, 73	1.54	–0.10	832.03	—
A90/2778	807C-6R-4, 73	1.66	0.04	833.53	—
A90/2779	807C-6R-5, 73	1.74	–0.08	835.03	—
A90/2780	807C-12R-1, 35	1.76	–0.10	876.95	—
A90/2781	807C-15R-1, 57	1.99	–0.66	894.47	—
A90/2782	807C-16R-1, 78	1.92	–0.80	899.68	—
A90/2783	807C-17R-1, 76	1.55	–0.73	904.66	—
A90/2784	807C-17R-2, 73	1.56	–0.62	906.13	—
A90/2785	807C-18R-CC, 2	1.63	–0.71	908.92	—
A90/2786	807C-19R-1, 55	1.75	–0.74	914.45	—
A90/2787	807C-20R-1, 1	1.86	–0.80	918.91	—
A90/2788	807C-21R-1, 12	2.07	–0.67	924.02	—
A90/2789	807C-22R-1, 12	1.98	–0.99	933.82	—
A90/2790	807C-23R-1, 64	2.06	–0.96	939.34	—
A90/2791	807C-23R-2, 64	2.11	–0.80	940.84	—
A90/2792	807C-23R-3, 64	2.26	–0.76	942.34	—
A90/2793	807C-23R-4, 16	2.22	–0.91	943.36	—
A90/2794	807C-24R-1, 73	2.29	–0.67	944.43	—
A90/2795	807C-24R-2, 74	2.13	–0.61	945.94	—
A90/2796	807C-25R-1, 70	2.22	–0.83	949.10	—
A90/2797	807C-26R-1, 73	2.52	–0.52	958.83	—
A90/2798	807C-29R-1, 16	2.13	–0.49	987.26	—
A90/2866	807C-30R-2, 27	1.98	–0.64	997.83	—
A90/2867	807C-31R-1, 8	2.13	–0.73	1006.58	—
A90/2868	807C-32R-1, 16	2.63	–1.02	1016.26	—
A90/2869	807C-33R-1, 2	2.20	–1.22	1025.42	—
A90/2870	807C-34R-1, 3	2.37	–1.15	1034.63	—
A90/2871	807C-35R-1, 34	1.95	–0.92	1044.64	—
A90/2872	807C-37R-1, 7	1.91	–0.97	1063.77	—
A90/2873	807C-38R-1, 4	2.12	–1.11	1073.64	—
A90/2874	807C-39R-1, 25	2.08	–1.03	1082.65	—
A90/2875	807C-40R-1, 45	1.69	–1.13	1092.45	—
A90/2876	807C-41R-1, 32	1.90	–1.25	1098.02	—
A90/2877	807C-42R-1, 74	1.99	–1.23	1103.14	—
A90/2811	807C-43R-1, 71	1.72	–1.77	1107.11	—
A90/2812	807C-44R-1, 76	1.81	–1.36	1116.76	—
A90/2813	807C-45R-1, 65	2.47	–1.58	1126.25	—
A90/2814	807C-45R-2, 64	1.27	–1.39	1127.74	—
A90/2815	807C-46R-1, 73	1.50	–1.39	1135.93	—
A90/2816	807C-46R-2, 74	1.44	–1.31	1137.44	—
A90/2817	807C-46R-3, 62	1.24	–0.89	1138.82	—
A90/2818	807C-47R-1, 70	1.49	–1.97	1140.90	—
A90/2819	807C-47R-2, 88	1.74	–1.96	1142.58	—
A90/2820	807C-48R-1, 20	1.83	–1.99	1145.40	—
A90/2821	807C-48R-2, 19	2.33	–1.93	1146.89	—
A90/2822	807C-49R-1, 22	2.06	–2.10	1150.42	—
A90/2823	807C-50R-1, 21	2.42	–2.23	1155.41	—
A90/2824	807C-51R-1, 21	3.04	–1.95	1160.41	—
A90/2825	807C-51R-2, 23	3.31	–1.99	1161.93	—
A90/2826	807C-51R-3, 119	3.13	–1.82	1164.39	—
A90/2827	807C-51R-4, 39	3.42	–2.04	1165.09	—
A90/2828	807C-52R-1, 20	3.52	–2.18	1170.00	—
A90/2829	807C-52R-2, 20	3.25	–1.97	1171.50	—
A90/2830	807C-52R-3, 19	3.14	–1.81	1172.99	—
A90/2831	807C-53R-1, 20	2.54	–1.71	1179.60	—
A90/2832	807C-53R-2, 20	1.74	–1.54	1181.10	—
A90/2833	807C-53R-3, 20	1.74	–1.77	1182.60	—
A90/2834	807C-53R-4, 20	1.79	–1.37	1184.07	—
A90/1936	807C-54R-1, 0	1.37	–1.73	1188.80	65.73
A90/1937	807C-54R-1, 15	1.34	–1.76	1188.95	65.74
A90/1938	807C-54R-1, 26	1.28	–1.73	1189.06	65.75
A90/1939	807C-54R-1, 35	1.31	–2.01	1189.15	65.76
A90/1940	807C-54R-1, 47	1.36	–1.95	1189.27	65.77
A90/1941	807C-54R-1, 56	1.44	–1.60	1189.36	65.77
A90/1942	807C-54R-1, 68	1.31	–1.78	1189.48	65.78
A90/1943	807C-54R-1, 85	1.74	–1.51	1189.65	65.80
A90/1944	807C-54R-1, 104	1.35	–1.69	1189.84	65.81
A90/1945	807C-54R-1, 117	1.30	–1.76	1189.97	65.82
A90/1946	807C-54R-1, 133	1.30	–1.80	1190.13	65.83
A90/1947	807C-54R-1, 146	1.60	–1.13	1190.26	65.84
A90/1948	807C-54R-2, 10	1.47	–1.75	1190.40	65.86

Appendix (continued).

Lab no.	Hole, core, section, interval (cm)	$\delta^{13}C$	$\delta^{18}O$	Depth (mbsf)	Age (Ma)	Lab no.	Hole, core, section, interval (cm)	$\delta^{13}C$	$\delta^{18}O$	Depth (mbsf)	Age (Ma)
A90/1949	807C-54R-2, 18	1.56	–1.26	1190.48	65.86	A90/2348	807C-55R-3, 85	2.35	–1.67	1200.75	66.67
A90/1950	807C-54R-2, 32	1.65	–1.35	1190.62	65.87	A90/2349	807C-55R-3, 103	2.45	–1.72	1200.93	66.68
A90/1951	807C-54R-2, 42	1.86	–1.51	1190.72	65.88	A90/2350	807C-55R-3, 112	2.50	–1.68	1201.02	66.69
A90/1952	807C-54R-2, 55	1.70	–1.63	1190.85	65.89	A90/2351	807C-55R-3, 124	2.52	–1.57	1201.14	66.70
A90/1953	807C-54R-2, 62	2.02	–0.78	1190.92	65.90	A90/2352	807C-55R-3, 133	2.54	–1.52	1201.23	66.71
A90/1954	807C-54R-2, 73	1.70	–1.69	1191.03	65.90	A90/2353	807C-55R-3, 143	2.26	–2.26	1201.33	66.72
A90/1955	807C-54R-2, 81	1.62	–1.52	1191.11	65.91	A90/2354	807C-55R-4, 11	2.39	–1.83	1201.51	66.73
A90/1956	807C-54R-2, 86	1.65	–1.49	1191.16	65.91	A90/2355	807C-55R-4, 21	2.54	–1.67	1201.61	66.74
A90/1957	807C-54R-2, 101	1.51	–1.75	1191.31	65.93	A90/2356	807C-55R-4, 37	2.72	–1.67	1201.77	66.75
A90/1958	807C-54R-2, 107	1.56	–1.69	1191.37	65.93	A90/2357	807C-55R-4, 49	2.66	–1.64	1201.89	66.76
A90/1959	807C-54R-2, 117	1.44	–1.32	1191.47	65.94	A90/2358	807C-55R-4, 63	2.67	–1.76	1202.03	66.77
A90/1960	807C-54R-2, 126	1.42	–1.45	1191.56	65.95	A90/2359	807C-55R-4, 73	2.69	–1.59	1202.13	66.78
A90/1961	807C-54R-2, 138	1.71	–1.71	1191.68	65.96	A90/2360	807C-55R-4, 85	2.85	–1.58	1202.25	66.79
A90/1962	807C-54R-2, 149	1.78	–1.72	1191.79	65.96	A90/2361	807C-55R-4, 98	2.75	–1.72	1202.38	66.80
A90/1963	807C-54R-3, 12	1.75	–1.87	1191.92	65.97	A90/2380	807C-55R-4, 110	2.45	–2.03	1202.50	66.81
A90/1964	807C-54R-3, 22	1.34	–1.66	1192.02	65.98	A90/2381	807C-55R-4, 120	2.54	–1.86	1202.60	66.82
A90/1965	807C-54R-3, 32	1.25	–1.68	1192.12	65.99	A90/2382	807C-55R-4, 130	2.64	–1.91	1202.70	66.82
A90/1966	807C-54R-3, 44	1.21	–1.84	1192.24	66.00	A90/2383	807C-55R-4, 141	2.67	–1.72	1202.81	66.83
A90/1967	807C-54R-3, 53	1.14	–1.55	1192.33	66.01	A90/2835	807C-56R-1, 20	2.75	–1.81	1206.80	67.15
A90/1968	807C-54R-3, 67	1.29	–1.68	1192.47	66.02	A90/2836	807C-56R-2, 20	2.87	–1.64	1208.30	67.26
A90/1969	807C-54R-3, 75	1.49	–1.64	1192.55	66.02	A90/2837	807C-56R-3, 20	2.79	–1.75	1209.80	67.38
A90/1970	807C-54R-3, 88	1.51	–1.69	1192.68	66.03	A90/2838	807C-57R-1, 21	3.01	–1.60	1216.51	67.91
A90/1971	807C-54R-3, 97	1.59	–1.83	1192.77	66.04	A90/2839	807C-57R-2, 21	3.03	–1.77	1218.01	—
A90/1972	807C-54R-3, 106	1.37	–1.72	1192.86	66.05	A90/2840	807C-58R-1, 20	3.09	–1.69	1222.70	—
A90/1973	807C-54R-3, 116	1.47	–1.14	1192.96	66.06	A90/2841	807C-59R-1, 34	2.85	–1.61	1232.54	—
A90/2014	807C-54R-3, 122	1.03	–1.74	1193.02	66.06	A90/2842	807C-59R-2, 46	2.92	–1.65	1234.16	—
A90/2015	807C-54R-3, 132	1.33	–1.61	1193.12	66.07	A90/2844	807C-61R-1, 110	2.96	–1.73	1252.60	—
A90/2016	807C-54R-3, 139	1.36	–1.93	1193.19	66.07	A90/2865	807C-61R-2, 112	2.95	–1.70	1254.12	—
A90/2017	807C-54R-3, 149	1.33	–1.86	1193.29	66.08	A90/2384	807C-62R-1, 35	2.87	–1.68	1261.55	—
A90/2018	807C-54R-4, 9	1.64	–1.68	1193.39	66.09	A90/2385	807C-62R-2, 34	2.92	–1.51	1263.04	—
A90/2019	807C-54R-4, 20	1.60	–1.72	1193.50	66.10	A90/2386	807C-62R-3, 41	2.90	–1.77	1264.61	—
A90/2020	807C-54R-4, 31	1.60	–1.95	1193.61	66.11	A90/2387	807C-63R-1, 81	3.04	–1.47	1271.61	—
A90/2021	807C-54R-4, 40	1.22	–1.81	1193.70	66.11	A90/2388	807C-63R-2, 81	3.01	–1.51	1273.11	—
A90/2022	807C-54R-4, 50	1.75	–1.72	1193.80	66.12	A90/2389	807C-63R-3, 81	2.98	–1.76	1274.61	—
A90/2023	807C-54R-4, 62	1.64	–1.87	1193.92	66.13	A90/2390	807C-63R-4, 85	3.01	–1.44	1276.15	—
A90/2024	807C-54R-4, 80	1.81	–1.74	1194.10	66.15	A90/2391	807C-64R-1, 121	3.01	–1.67	1281.71	—
A90/2025	807C-54R-4, 90	1.70	–1.85	1194.20	66.15	A90/2392	807C-64R-2, 121	2.97	–1.72	1283.21	—
A90/2026	807C-54R-4, 100	1.52	–1.46	1194.30	66.16	A90/2393	807C-64R-3, 39	2.88	–1.74	1283.89	—
A90/2027	807C-54R-4, 113	1.69	–1.76	1194.43	66.17	A90/2394	807C-65R-1, 58	3.01	–1.80	1290.68	—
A90/2028	807C-54R-4, 125	1.83	–1.86	1194.55	66.18	A90/2395	807C-65R-2, 60	3.10	–1.67	1292.20	—
A90/2029	807C-54R-4, 135	1.84	–1.10	1194.65	66.19	A90/2396	807C-66R-1, 55	3.17	–1.71	1300.35	—
A90/2030	807C-54R-4, 148	1.76	–1.65	1194.78	66.20	A90/2397	807C-66R-2, 55	3.14	–1.74	1301.85	—
A90/2031	807C-55R-1, 7	1.89	–1.60	1196.97	66.37	A90/2398	807C-66R-3, 55	3.08	–1.83	1303.35	—
A90/2032	807C-55R-1, 17	2.05	–1.81	1197.07	66.38	A90/2399	807C-67R-1, 132	2.92	–1.86	1310.82	—
A90/2033	807C-55R-1, 26	2.20	–1.51	1197.16	66.39	A90/2400	807C-67R-2, 132	2.98	–1.76	1312.26	—
A90/2034	807C-55R-1, 35	2.06	–1.89	1197.25	66.39	A90/2401	807C-67R-3, 132	2.97	–1.82	1313.76	—
A90/2035	807C-55R-1, 49	2.08	–1.80	1197.39	66.41	A90/2402	807C-67R-4, 125	3.04	–1.72	1315.19	—
A90/2036	807C-55R-1, 65	2.10	–1.62	1197.55	66.42	A90/2403	807C-67R-5, 47	2.94	–1.83	1315.91	—
A90/2037	807C-55R-1, 76	2.00	–1.75	1197.66	66.43	A90/2404	807C-68R-1, 77	2.92	–1.79	1319.87	—
A90/2039	807C-55R-1, 97	2.04	–1.78	1197.87	66.44	A90/2405	807C-68R-2, 50	3.04	–1.68	1321.10	—
A90/2041	807C-55R-1, 118	2.03	–1.81	1198.08	66.46	A90/2406	807C-68R-3, 26	3.07	–1.66	1322.36	—
A90/2042	807C-55R-2, 12	2.04	–1.91	1198.52	66.49	A90/2407	807C-69R-1, 58	3.05	–1.71	1329.38	—
A90/2043	807C-55R-2, 22	2.01	–1.74	1198.62	66.50	A90/2408	807C-69R-2, 56	3.04	–1.76	1330.86	—
A90/2045	807C-55R-2, 34	2.27	–1.69	1198.74	66.51	A90/2409	807C-69R-3, 57	3.07	–1.70	1332.37	—
A90/2046	807C-55R-2, 43	2.10	–1.57	1198.83	66.52	A90/2487	807C-69R-4, 65	3.07	–1.97	1333.95	—
A90/2047	807C-55R-2, 50	2.17	–1.80	1198.90	66.52	A90/2488	807C-69R-5, 70	3.17	–1.85	1335.50	—
A90/2048	807C-55R-2, 56	2.20	–1.67	1198.96	66.53	A90/2489	807C-70R-1, 46	3.15	–2.03	1338.86	—
A90/2049	807C-55R-2, 64	2.23	–1.66	1199.04	66.54	A90/2490	807C-70R-2, 89	3.25	–1.89	1340.79	—
A90/2050	807C-55R-2, 77	2.20	–1.47	1199.17	66.55	A90/2491	807C-70R-3, 9,	3.21	–1.95	1341.49	—
A90/2342	807C-55R-3, 12	2.25	–1.68	1200.02	66.61	A90/2492	807C-70R-4, 75	3.22	–1.94	1343.65	—
A90/2343	807C-55R-3, 30	2.31	–1.60	1200.20	66.63	A90/2493	807C-70R-5, 28	3.19	–1.77	1344.68	—
A90/2344	807C-55R-3, 38	2.24	–1.68	1200.28	66.63	A90/2494	807C-71R-1, 67	3.17	–1.85	1348.67	—
A90/2346	807C-55R-3, 51	2.33	–1.83	1200.41	66.64	A90/2495	807C-71R-2, 36	3.10	–2.02	1349.86	—
A90/2345	807C-55R-3, 59	2.36	–1.73	1200.49	66.65	A90/2496	807C-71R-3, 28	3.12	–1.84	1351.28	—
A90/2347	807C-55R-3, 71	2.46	–1.56	1200.61	66.66						